

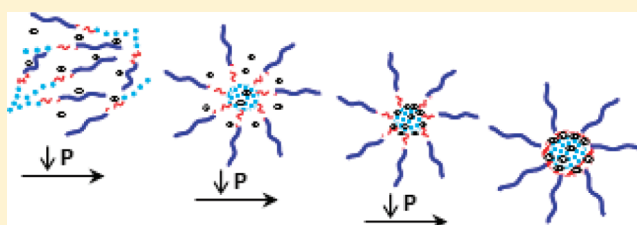
Multilayered Nanoparticles for Controlled Release of Paclitaxel Formed by Near-Critical Micellization of Triblock Copolymers

Zachary L. Tyrrell,[†] Youqing Shen,^{*,‡} and Maciej Radosz^{*,†}

[†]Soft Materials Laboratory, Department of Chemical & Petroleum Engineering, University of Wyoming, Laramie, Wyoming 82071, United States

[‡]Center for Bionanoengineering and the State Key Laboratory of Chemical Engineering, Zhejiang University, Hangzhou, China 310027

ABSTRACT: Near-critical micellization (NCM), allowing for precise pressure-tuned control of sequential block collapse and micelle formation, can be synchronized with cancer-drug encapsulation with virtually no drug losses. NCM is demonstrated to produce benign, stable nanoparticles made of PEG-*b*-PLLA-*b*-PCL triblock copolymers that are not only solvent-free and paclitaxel-rich, which reduces the body exposure to the excipients, but also nearly burst-release-free, which reduces if not eliminates its toxic side effects while enhancing its therapeutic efficacy.



INTRODUCTION

Drug carriers made of micelles of simple amphiphilic diblock copolymers, such as PEG-*b*-PLA micelles loaded with the hydrophobic cancer drug paclitaxel,¹ are well-known and promising enough to undergo phase III clinical tests because, in general, they can be more benign than the powerful but nonspecific free drug itself.^{2–9} This way, a higher fraction of therapeutically productive drug ends up in the cancer tissue, as intended, instead of the healthy tissues, which alleviates the side effects relative to the free drug treatment. This therapeutically productive drug fraction could be even higher, and conversely, the counterproductive, toxic fraction could be even lower, if not for an excessive release of the initial drug fraction immediately following application. Such an undesirable “burst release”, a persistent fingerprint of most diblock micellar carriers, except for those that are plagued by low drug loading to begin with, significantly inhibits the probability of their clinical success.^{10–13} The root cause of burst release lies in the process of loading the drug into the micelles. Generally, both the drug and the block copolymer are dissolved in a water-miscible organic solvent, and then water, the selective antisolvent for the drug and hydrophobic block, is added to induce both drug nucleation and micelle formation.¹⁴ The popular but naively simplistic view is that both of these distinct phenomena occur simultaneously and the drug is encapsulated in the core of the micelles.^{15,16} However, this is not the case. A large fraction of the drug is actually adsorbed on the core surface, resulting in burst release.¹⁷ Subtle differences in the exact sequence of micellization and drug nucleation can prevent drug from reaching inside the core, which instead ends up trapped in the micelle corona on its way to the core, and hence have little resistance to be released prematurely. Regardless of its exact distribution within and around the core, and how it may affect

the release rates, the pressing challenge is to find a robust and easily approvable approach to protecting the drug from burst release, recognized as one of the keys to increasing therapeutic efficacy of drug loaded micelles.¹⁸

There have been numerous known attempts to suppress burst release via new structures such as cross-linking of the micelle core or shell,¹⁹ conjugating drugs to the core,^{20,21} or even imparting an exotic protective layer designed to respond to external stimulus, such as pH^{17,22} or heat.^{23,24} However, such complicated modifications are hardly robust, not to mention a long and uncertain approval process they face. By contrast, the common blocks, such as PCL, PLA, and PEG, have all been approved for clinical use in other formulations,^{1,25} and in fact, PEG-PLA micelles loaded with paclitaxel are in phase III clinical trials (ClinicalTrials.gov), despite their serious burst-release problems. Our goal, therefore, is to develop a translatable drug-loading process that can use these FDA-approved building blocks to fabricate drug-loaded micelles with minimized burst release and hence mitigate its side effects while enhancing its therapeutic efficacy.

We previously developed a near-critical micellization (NCM) method and fabricated PEG-PCL micelles loaded with paclitaxel.²⁶ The resulting micelles had much high drug loading but did little to reduce burst release. We thus further hypothesized that adding a protective layer on the drug-containing core should reduce the burst-release probability. In principle, this can be accomplished with a suitable multiblock (at least triblock) copolymer via a precisely controlled sequential collapse of the blocks. Such a precise sequential

Received: February 8, 2012

Revised: May 14, 2012

Published: May 24, 2012

block collapse, carefully synchronized with drug nucleation and encapsulation, is hard or impossible with the conventional liquid-solvent-antisolvent micellization method but it is attainable with the NCM method. This is because, instead of low-resolution, hard-to-control liquid solvents, the NCM method relies on compressed, near-critical gases that allow for precise, pressure-tuned control of each crucial structure-forming stage separately, including micelle formation, drug nucleation, and encapsulation, then separately again, the protective layer formation upon the collapse of the middle block, as qualitatively illustrated in Figure 1, and, finally, corona

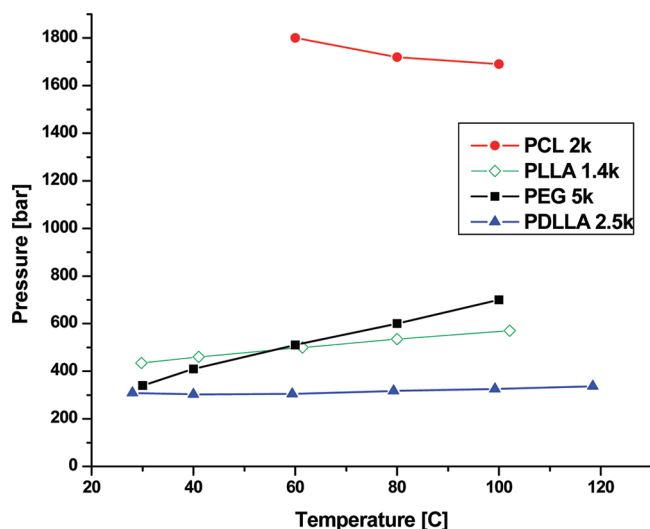


Figure 1. Cloud points in trifluoromethane of polycaprolactone (MW 2000), poly(L-lactide) (MW 1400), poly(ethylene glycol) (MW 5000), and poly(D,L-lactide) (MW 2500). The concentrations of the polymers are 1 wt %.

collapse that triggers particle separation from the solvent. The particles formed in this manner are collected simply by rapid decompression of the solvent, which exists as a gas at ambient conditions and hence leaves no residual solvent traces.

Our specific aim is to prove this hypothesis using ABC-type triblock copolymers with poly(ethylene glycol) (PEG) as the hydrophilic, corona-forming block on one end, poly(ϵ -caprolactone) (PCL) as the hydrophobic, core-forming block on the other end, and a middle block that should form a protective “shell” around the core. For this auxiliary middle block, we select two models: poly(L-lactide) (PLLA), which is crystallizable (crystallinity around 37%, a glass transition temperature around 60–65 °C, a melting temperature between 173 and 178 °C), and poly(D,L-lactide) (PDLLA), which is amorphous.²⁷ A structurally analogous reference diblock is PEG-*b*-(PDLLA-*co*-PCL), with a hydrophobic segment made of randomly distributed D,L-lactide and ϵ -caprolactone monomers. Our proof of concept will require characterizing all these micellar nanoparticles for drug loading content, drug encapsulation efficiency, overall drug loading efficiency, and drug release kinetics in water.

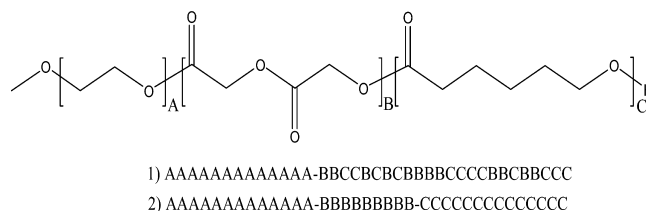
■ APPROACH

Materials. Methoxypoly(ethylene glycol), ϵ -caprolactone, D,L-lactide (3,6-dimethyl-1,4-dioxane-2,5-dione), and stannous octoate (Sn(Oct)₂) were obtained from Sigma-Aldrich. Polycaprolactone and poly(D,L-lactide) were obtained from Polymer Source, Inc. Dimethyl ether and trifluoromethane were obtained from Airgas at 99.5% purity.

Polymer Synthesis. PEG-*b*-(PDLLA-*co*-PCL) was synthesized in a manner consistent with the literature.²⁸ Briefly, synthesis was accomplished by ring-opening polymerization of ϵ -caprolactone and D,L-lactide initiated by PEG-OH (5K) in the presence of stannous octoate (0.05 wt %) in a polymerization tube under nitrogen. The polymerization tube was placed in an oil bath at 160 °C for 3 h. The product was extracted using dichloromethane, precipitated with cold methanol, and then dried under vacuum for 48 h.

PEG-*b*-PDLLA-*b*-PCL and PEG-*b*-PLLA-*b*-PCL were synthesized in two steps using a similar procedure. Polymer structures used in this

Scheme 1. Structure of Multiblock Copolymers Used in This Work^a



^aNote: 1) corresponds to the diblock PEG-*b*-(PDLLA-*co*-PCL) and 2) corresponds to the triblocks PEG-*b*-PDLLA-*b*-PCL and PEG-*b*-PLLA-*b*-PCL, with the sole difference being that PDLLA contains both D- and L-isoforms of the monomer while PLLA contains only L-isoforms.

work are summarized in Scheme 1. For PEG-*b*-PDLLA-*b*-PCL, first, PEG-*b*-PDLLA-OH was synthesized by ring-opening polymerization of D,L-lactide initiated by PEG-OH (5K) in the presence of Sn(Oct)₂ catalyst in a polymerization tube under nitrogen and placed in an oil bath at 145 °C for 3 h. PEG-*b*-PDLLA was recovered by extracting with dichloromethane, precipitated with cold methanol, and dried under vacuum for 48 h to remove residual solvent. Second, PEG-*b*-PDLLA-*b*-PCL was synthesized by ring-opening polymerization of ϵ -caprolactone initiated by PEG-*b*-PDLLA-OH in the presence of Sn(Oct)₂ catalyst in a polymerization tube under nitrogen and placed in an oil bath at 160 °C for 3 h. The product was extracted with dichloromethane, precipitated with cold methanol, and dried under vacuum for 48 h. Molecular weight and structure were determined by NMR, and molecular weight and polydispersity index (PDI) were confirmed by GPC.

Cloud Point Measurements. The cloud point refers to the onset of a bulk transition of a binary solution from a homogeneous one-phase region to a heterogeneous two-phase region. The cloud point transition for systems studied in this work can be induced either by decreasing temperature at constant pressure, which results in the cloud temperature, or by decreasing pressure at constant temperature, which results in the cloud pressure (CP). Upon increasing pressure or temperature beyond the cloud point boundary, the solution returns to its homogeneous one-phase state. The micellization pressure (MP) refers to the highest pressure at which micelles can be formed in a homogeneous solution upon decompression or, conversely, decomposed upon compression, at constant temperature. The nanosized micelle-containing phase is referred to as the micellar solution, in contrast to the molecular solution observed following micelle decomposition.

The CP and MP transitions are measured in a small (about 1 cm³ in volume) high-pressure variable-volume cell coupled with transmitted- and scattered-light intensity probes and with a borescope for visual observation of the phase transitions. This apparatus is equipped with a data acquisition and control systems that allow not only for constant temperature and pressure measurements but also for decreasing and increasing temperature and pressure measurements at a constant rate. The cloud points reported in this work are detected with a transmitted-light intensity probe. The micellization points are detected with a scattered-light intensity probe. A more detailed description of

the apparatus and of its transmitted- and scattered-light intensity probes is given elsewhere.²⁹

A known amount of the copolymer that will typically lead to a 1.0 wt % solution and solvent are loaded into the cell, which is then brought to and maintained at a desired pressure and temperature at which copolymer can be dissolved. Upon decompression, the bulk phase boundary (e.g., CP) is approached from the one-phase or micellar phase side, and the transmitted light intensity (TLI) starts decreasing. Conversely, upon compression, the phase boundary is approached from the two-phase side, and TLI starts increasing. A new data point is taken after equilibrating the mixture for 15 min in the one-phase region, well above the expected cloud temperature and pressure. In all cases, the TLI data are stored and analyzed as a function of time, temperature, and pressure. The cloud pressure in this work is taken as the inflection point on the TLI curve, which corresponds to a peak on its first derivative.

Micelle formation is probed using high-pressure dynamic light scattering. The scattered light intensity and the hydrodynamic radius sharply increase on approaching the micellization pressure from the high-pressure side. For these measurements, we couple our high-pressure equilibrium cell with an argon ion laser (National Laser) model 800BL operating at wavelength of 488 nm and a Brookhaven BI-9000AT correlator, as described previously.²⁹

Nanoparticle Preparation. Aqueous drug-loaded micelle solutions are prepared by the following procedure. The polymer, drug, and selected solvent (trifluoromethane, dimethyl ether, or a mixture of the two) are loaded into the high-pressure cell. The solvent composition is chosen based on the relative phase behavior of the drug and the polymer. The polymer and drug are dissolved by setting the temperature and pressure well into the one-phase region, again determined from the phase diagrams of the polymer solution alone and the drug solution alone. Upon dissolution, the temperature is lowered to 35 °C at constant pressure, and the mixture is equilibrated for 15 min. The pressure is then lowered slowly (10 bar/min) to within 50 bar of the cloud point for the mixture to allow adequate time for the equilibration of the micellization process. From this point, the mixture is rapidly depressurized by releasing the pressurizing fluid (propane). The polymer is precipitated as the solvent rapidly evaporates. The solvent is then released slowly from the cell to prevent the loss of solids. The cell is washed with a known volume of distilled water into a flask and stirred. The volume of water is chosen to give a final concentration of 0.1 wt % polymer.

Particle Size. Particle size measurements of the aqueous solutions are performed using dynamic light scattering after filtering the solution with a 0.2 μm PTFE filter.

Critical Micelle Concentration. Critical micelle concentration (CMC) is measured by two methods. First, particle size of aqueous solutions is measured upon dilution at defined concentration intervals. The CMC is the point at which the particle size drops significantly, more than 30%. Once the CMC is approximated by this method, a second method is used for confirmation and higher resolution at low concentrations, as described previously in the literature.³⁰ Briefly, aqueous micelle solutions are prepared with pyrene, which partitions between the micelle cores and solution. The partition coefficient can be determined by measuring the fluorescence spectra of the solution over a range of wavelengths and comparing the relative intensity of specific fluorescence intensity peaks. These peaks correspond to pyrene fluorescence in a hydrophobic microenvironment and a hydrophilic microenvironment. When the concentration falls below the CMC, the hydrophobic intensity peak, and hence the partition coefficient, changes abruptly.

Drug Loading. Drug loading is characterized by the drug loading content (DLC), the drug encapsulation efficiency (DEE), and the drug loading efficiency (DLE) defined as follows:

$$\text{DLC} = \frac{\text{weight of drug in micelles}}{\text{total weight of micelles}} \times 100\%$$

$$\text{DEE} = \frac{\text{weight fraction drug in micelles}}{\text{initial weight fraction of drug}} \times 100\%$$

$$\text{DLE} = \frac{\text{weight of drug in micelles}}{\text{initial weight of drug}} \times 100\%$$

Drug loading content represents the weight fraction of the drug captured in the micelles after processing. We define two separate efficiencies in order to more precisely pinpoint the cause of drug losses in the process. Drug loading efficiency represents an overall process efficiency and accounts for all sources of drug loss, including inefficient encapsulation, filtering losses, and transfer losses. Calculation of drug encapsulation efficiency simply removes the losses due to filtering and transfer, so the actual encapsulation process can be quantified.

Prior to determination of drug loading content, all drug-loaded micelle solutions are filtered through a 0.2 μm PTFE filter to remove any crystallized, unencapsulated drug. The amount of drug in the micelles is measured with HPLC using a mobile phase mixture of acetonitrile and water with a gradient starting at 50% acetonitrile and ending at 90% acetonitrile, through a Hypersil ODS 5 mm column (Agilent), with a flow rate of 1 mL/min. UV-absorbance is monitored at a wavelength of 225 nm for paclitaxel. Drug concentration is determined by calibration with a series of standards of known concentration. The total weight of the micelles is determined by removing water from the aqueous solution and weighing the sample. Experiments are repeated 3–5 times to confirm accuracy. This method is consistent with that reported previously.²⁶

Drug Release. 3 mL of aqueous drug-loaded micelle solution is placed in a dialysis cartridge (MWCO 3500, Fisher Scientific), which is then placed in 200 mL of distilled water in a beaker, adjusted to a pH of 7.4 by Na₂CO₃, and held at a constant temperature of 37 °C in a water bath with horizontal shaking. The pH is monitored over the duration of the experiment to ensure that it remains constant. At defined time intervals, a sample of 100 μL is taken from the dialysis cartridge and mixed with the same volume of acetonitrile. The drug concentration is then measured using HPLC.

RESULTS AND DISCUSSION

Polymer Phase Behavior. As a frame of reference, the cloud pressures of the corresponding homopolymers, PEG (MW 5000), PCL (MW 2000), and PDLLA (MW 2500) in trifluoromethane are shown in Figure 1. The cloud pressures for PCL are much higher than those for PEG, PLLA, and PDLLA, suggesting trifluoromethane is a relatively weak solvent for PCL and a relatively strong solvent for PEG, PLLA, and PDLLA. Although trifluoromethane has similar solvent capacities for PEG, PLLA, and PDLLA, upon closer inspection, there are significant differences to note. In the temperature range most relevant to preparing drug loaded micelles, namely 20–40 °C, the cloud pressure of PLLA is higher than that of PEG, by about 75 bar at 30 °C, whereas the cloud pressure of PDLLA is lower than PEG, by about 25 bar at 30 °C. Since the relationship between the cloud pressures of the homopolymers in dimethyl ether, the less selective solvent component, is similar, the results are not shown.

As reported previously,³¹ for a simple diblock formed from blocks which, as homopolymers, exhibit a large difference in cloud pressure, as is the case for PEG and PCL, the result manifests itself in a cloud pressure and a micellization pressure that fall between the cloud pressures of the individual homopolymers. The micellization pressure is result of the less soluble block aggregating together, but being unable to coalesce and precipitate in bulk due to the attachment of the more soluble block, and hence, the micellization occurs below but not

too far from the cloud pressure of the less soluble block. As the pressure is lowered, the corona collapses that causes the onset of copolymer precipitation at its cloud pressure, which is closer to the cloud pressure of the more soluble block.

This type of behavior is illustrated with a new, relevant to this work example in Figure 2, showing the cloud pressure of PEG-

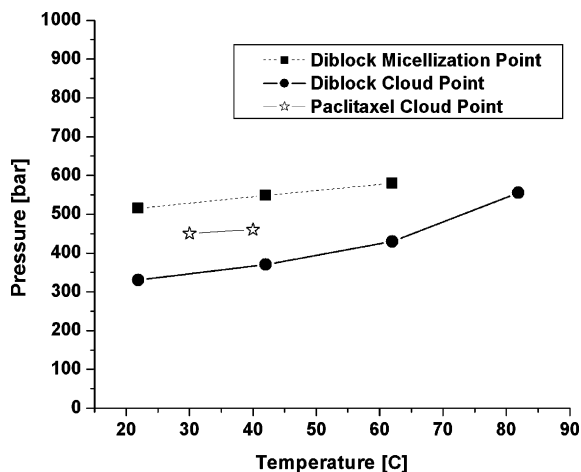


Figure 2. Cloud points and micellization points of PEG-*b*-[PDLLA-*co*-PCL] (MW 5K-*b*-(2K-*co*-3K)) and cloud points of paclitaxel in 50% trifluoromethane/50% dimethyl ether. Polymer and drug concentrations are 2 and 0.2 wt %, respectively.

b-(PCL-*co*-PDLLA) in a 50/50 mixture of trifluoromethane and dimethyl ether. In this case, the less soluble, core-forming block is a random copolymer of PCL and PDLLA, and the more soluble, corona-forming block is PEG. This solvent composition (50/50) is convenient because it leads to an easily attainable and robust micellar region, around 300–500 bar between 30 and 40 °C, typical of compressible micellar solutions of other diblock copolymers.^{14,29,31,32} More important, this solvent also allows for the cloud pressure of paclitaxel (shown with stars), and hence the onset of its nucleation, to fall within this micellar region, which is auspicious for effective encapsulation.

Multilayered Micelle Formation. For each triblock copolymer, PEG-*b*-PDLLA-*b*-PCL or PEG-*b*-PLLA-*b*-PCL, in a suitable compressible fluid, for example a mixture of trifluoromethane and dimethyl ether, one can qualitatively predict the initial and final transition upon decompression of its initially homogeneous solution, namely that the least soluble block, PCL, will aggregate first to form micelles at the micellization pressure (MP), and that eventually the entire copolymer will bulk phase separate at the cloud pressure (CP), upon the collapse of the last block, just as is the case for a diblock. If that is the case, then the intermediate block, either the middle block or PEG, must also collapse in an attempt to phase separate at its distinct intermediate pressure, certainly between MP and CP, just as the other two blocks of the copolymer do. For example, for PEG-*b*-PLLA-*b*-PCL, based on the cloud pressures of the individual blocks shown in Figure 1, the expected order of the transitions upon decreasing pressure at room temperature should be, first, aggregation of the least soluble block, PCL, followed by collapse of the middle block, PLLA, on the already formed micelle core, and, finally, collapse of the ultimate corona-forming block, PEG, at the onset of bulk phase separation. However, if PDLLA is substituted for PLLA,

as in PEG-*b*-PDLLA-*b*-PCL, the cloud pressure of the middle block alone (PDLLA as a homopolymer shown in Figure 2) now lies somewhat below the cloud pressure of PEG. In this case, therefore, PEG should collapse first, before PDLLA does (at the onset of inevitable bulk phase separation).

Approximate analysis of scattered light intensity upon decreasing pressure is used to explore such block-collapse-induced transitions for both triblocks, PEG-*b*-PDLLA-*b*-PCL and PEG-*b*-PLLA-*b*-PCL, where we expect three transitions, and for the corresponding diblock PEG-*b*-(PDLLA-*co*-PCL), where we expect only two transitions. Figure 3 compares the

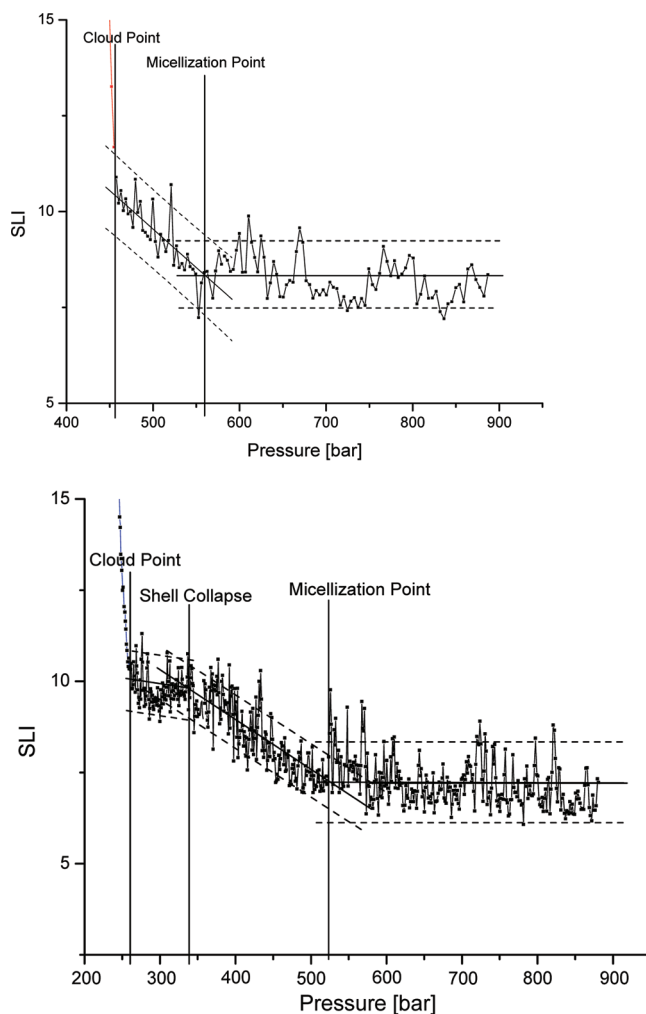


Figure 3. Scattered light intensity as a function of pressure for PEG-*b*-(PDLLA-*co*-PCL), upper trace, and PEG-*b*-PLLA-*b*-PCL, lower trace, both in 50% trifluoromethane/50% dimethyl ether. Temperature is 40 °C and polymer concentration 2 wt % for both polymers.

scattered light intensity plotted as a function of pressure for PEG-*b*-PLLA-*b*-PCL (lower trace) and PEG-*b*-(PDLLA-*co*-PCL) (upper trace). The distinct changes of slope on going from high pressure to low pressure for the triblock are attributed to the three transitions, namely, core aggregation at micellization pressure, middle layer collapse, and corona collapse immediately followed by bulk phase separation at cloud pressure. In order to establish a rough but somewhat consistent method of quantifying such transitions, which is nontrivial considering the inherently noisy data at such high pressures, one can use a simple statistical analysis based on

linear averaging. First, a baseline is established for the system in a one-phase homogeneous region by gathering scattered light data at a constant pressure within this region. Assuming safely that there is no substantial change in the average particle size upon decreasing pressure in the absence of a phase transition (the change, if any, is small), a horizontal line is drawn along with 90% confidence intervals established by this baseline measurement. Next, the point at which 90% of the data no longer fall within this confidence interval starts a new linear slope with 90% confidence interval that continues to lower pressures. Once the data begin to fall substantially outside of the new confidence interval, a new slope begins. In this manner, we reduce the data to approximate but distinct linear intervals that help quantify the pressures at which these transitions occur. Testing this simple analysis against reliable, previously reported phase transition data for a diblock of PEG-*b*-PCL³³ confirms that this method yields reasonable micellization and cloud pressures, within the experimental error limits. Therefore, we use this approach to quantify MP, CP, and the intermediate-block collapse pressure for our triblocks and the corresponding diblock.

The results are summarized in Figure 4 for PEG-*b*-PDLLA-*b*-PCL (MW 5000-*b*-1500-*b*-1500) in a 60/40 (w/w) mixture of

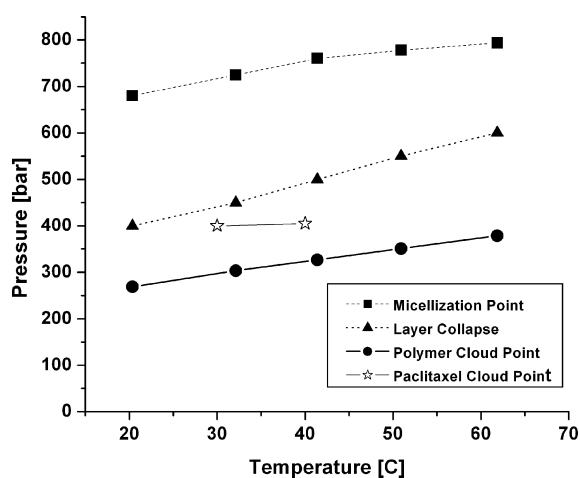


Figure 4. Cloud points and micellization points of PEG-*b*-PDLLA-*b*-PCL (MW 5000-*b*-1500-*b*-1500) and cloud points of paclitaxel in 60% trifluoromethane/40% dimethyl ether. Polymer and drug concentrations were 1.5 and 0.15 wt %, respectively.

trifluoromethane and dimethyl ether and in Figure 5 for PEG-*b*-PLLA-*b*-PCL (MW 5000-*b*-1500-*b*-1500) in 50/50 (w/w) trifluoromethane and dimethyl ether. In both cases, we observe the usual MP curve (top) and CP curve (bottom), but also an intermediate curve that corresponds to the intermediate-block collapse that causes the middle layer formation. In addition, the paclitaxel CP curves, measured in the absence of the block copolymer, are superimposed on Figures 4 and 5 as a crucial point of reference.

The solvents used in these experiments are slightly different (hence paclitaxel CP's are slightly different), as they were a priori optimized to coordinate micellization and each intermediate-block collapse with the paclitaxel cloud pressure, but no effort is made to readjust them a posteriori to make it exact. In the case of the PDLLA triblock; therefore, the cloud pressure of paclitaxel alone falls close to but below the middle layer collapse pressure, which means that paclitaxel nucleation

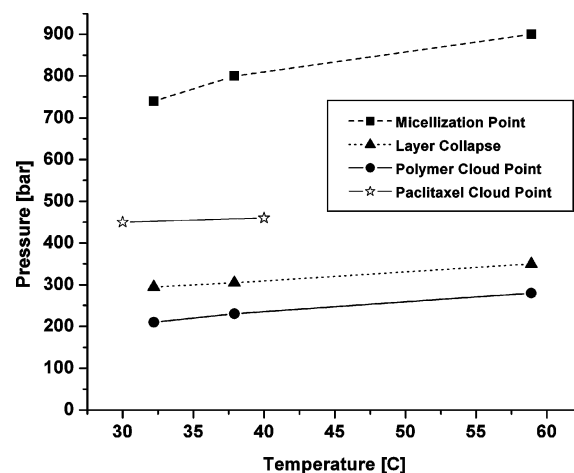


Figure 5. Cloud points and micellization points of PEG-*b*-PLLA-*b*-PCL (MW 5000-*b*-1500-*b*-1500) and cloud points of paclitaxel in 50% trifluoromethane/50% dimethyl ether. Polymer and drug concentrations were 1.5 and 0.15 wt %, respectively.

may follow or essentially coincide with the middle layer formation. For the PLLA triblock, by contrast, the cloud pressure of paclitaxel falls above the middle layer collapse pressure, which means that paclitaxel nucleation most likely precedes the middle layer formation. This difference alone, and its consequences, is worth reflecting on.

Toward this end, after the cloud pressures and micellization pressures are measured in appropriate solvent mixtures, the drug-loaded micelles are separated from the solvent by depressurization and redispersed in water. Their water suspensions are characterized by measuring particle size, drug loading content, drug loading efficiency, drug encapsulation efficiency, and drug release kinetics. It goes without saying that the original particle structure can be altered or completely destroyed by dispersion in a different solvent. However, in this case, we hypothesize that the original structure is largely preserved.³¹ While not proven directly, this is reasonable because the virgin block copolymers and the drug itself are essentially immiscible with water, and hence there is no way for them on their own to form from scratch any structures in water alone, while the material recovered from the near-critical micellization is easily and completely dispersible in water.

Size Distribution. Even more reassuring is to find that such water-dispersed particles have narrow size distribution around physically meaningful averages. Figure 6 shows the particle size distributions of PEG-*b*-(PDLLA-*co*-PCL), PEG-*b*-PDLLA-*b*-PCL, and PEG-*b*-PLLA-*b*-PCL. The PDLLA-containing triblock turns out to have the largest average particle size, 82 nm, despite having the same molecular weight as the PLLA-containing triblock, and a lower molecular weight than the diblock, which have average particle sizes of 74 and 72.2 nm, respectively. While the differences are small, the micelles formed from the PDLLA-containing triblock seem to be less compact than those of the micelles formed from the diblock or the PLLA-containing triblock, which can perhaps suggest a less compact middle layer, which may or may not be due to PLLA crystallizability, but this finding is consistent with the possibility of more crystallizable and hence tighter PLLA structure.

Drug Loading Content. For all three polymers, drug loading content is found to be much higher than that obtained from the conventional liquid method (only about 2% for a PEG-*b*-PCL diblock¹⁹). By contrast, as reported in Table 1, the

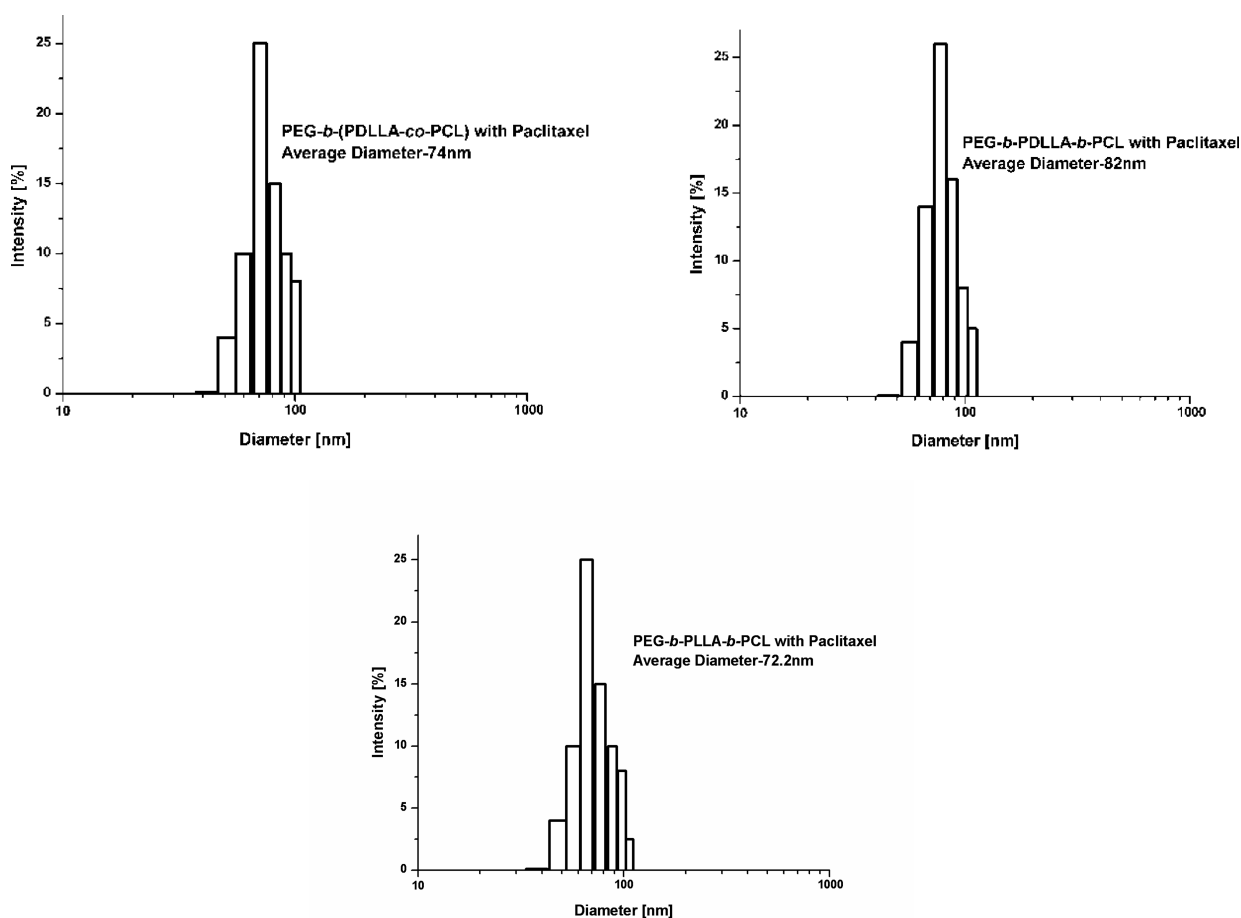


Figure 6. Particle size distributions of PEG-*b*-(PDLLA-*co*-PCL) [MW 5000-*b*-(2000-*co*-3000)], PEG-*b*-PDLLA-*b*-PCL [MW 5000-*b*-1500-*b*-1500], and PEG-*b*-PLLA-*b*-PCL [MW 5000-*b*-1500-*b*-1500] in water loaded with Paclitaxel. Average diameters: 74.0, 82.0, and 72.2 nm, respectively.

Table 1. Molecular Weight (MW), Critical Micelle Concentration (CMC), and Drug Loading Content and Efficiencies of the Diblock and Triblock Copolymers

polymer	MW	CMC ($\mu\text{mol/L}$)	loading content (%)	encapsulation efficiency (%)	overall loading efficiency (%)
PEG- <i>b</i> -(PDLLA- <i>co</i> -PCL)	5K-(2K- <i>co</i> -3K)	2.0	10.5	100	80.2
PEG- <i>b</i> -PDLLA- <i>b</i> -PCL	5K-1.5K-1.5K	0.5	10.9	106	72.3
PEG- <i>b</i> -PLLA- <i>b</i> -PCL	5K-1.5K-1.5K	0.05	10.4	98.6	77.1

drug loading contents for PEG-*b*-(PDLLA-*co*-PCL), PEG-*b*-PDLLA-*b*-PCL, and PEG-*b*-PLLA-*b*-PCL are found to be 10.5, 10.9, and 10.4 wt %, respectively, which is another illustration that precisely controlled near-critical micellization can consistently produce higher drug loading.²⁶ While not crucial to this study, such high drug loading contents are very desirable therapeutically as they drastically reduce the body exposure to the excipient polymer matter.

Encapsulation Efficiency. As also reported in Table 1, encapsulation efficiencies for all these polymers are also very high, 100%, 106% (which is possible the way we estimate it), and 98.6%, respectively, and overall drug loading efficiencies are 80.2%, 72.3%, and 77.1%, at least by a factor of 2 or 3 higher than those normally expected from the conventional liquid-processing method.¹⁴ This, in turn, suggests much lower processing losses of the extremely expensive cancer drug, which happens to be in short supply these days. Comparing the encapsulation efficiency with the calculated overall drug loading efficiency, the drug losses implied in the calculated drug loading efficiency are therefore an expected result of inefficiencies in the

transfer of the drug-loaded micelles resulting in loss of polymer and drug, rather than inefficient encapsulation. This is an important distinction because the transfer losses are expected to be eliminated upon scale-up, which means that the overall loading efficiencies should approach the encapsulation efficiencies (100%). Also exciting, this highly efficient encapsulation suggests a thermodynamically feasible and intriguing possibility that even higher drug loading content, which is desirable from the therapeutic standpoint, could be achieved by simply increasing the initial ratio of drug to polymer.

Drug Release Kinetics. Having characterized the particle size and drug loading, in this special case, it is illuminating and profitable to consider drug release kinetics as a rough measure of the drug-containing particle stability in a different but relevant solvent (it is well-known that in-*vivo* release may or may not be different, but this is a common preliminary approximation). Figure 7 shows the cumulative release of paclitaxel as a function of time into distilled water at pH 7.4, according to a commonly used approach for such particles.

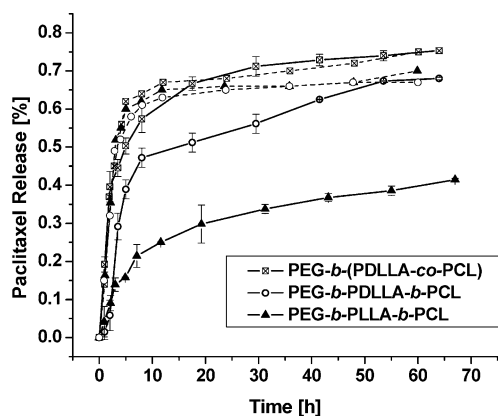


Figure 7. Cumulative paclitaxel release as a function of time for a diblock, PEG-*b*-[PDLLA-*co*-PCL] [MW 5000-*b*-(2000-*co*-3000)], and two triblocks: PEG-*b*-PDLLA-*b*-PCL [MW 5000-*b*-1500-*b*-1500] and PEG-*b*-PLLA-*b*-PCL [MW 5000-*b*-1500-*b*-1500] in distilled water at pH = 7.4 and $T = 37^\circ\text{C}$. Solid lines represent micelles prepared by near-critical micellization while dashed lines represent micelles prepared conventionally by solvent evaporation.

Upon going from the diblock (upper curve) to the PDLLA triblock (middle curve) to the PLLA triblock (lower curve), one observes a significant decrease of cumulative release. Furthermore, all three systems show some degree of decrease in the cumulative release when compared to micelles prepared conventionally by solvent evaporation. More important than the overall decrease is the manner in which the decrease is achieved, especially in the first few hours of the experiment, which suggests that burst release is reduced to the point of being eliminated upon introduction of the protective layer. This is significant because in order to be an effective drug delivery vehicle, the micelles must not release drug too quickly, as this will lead to nonspecific, systemic exposure to the drug, increasing the likelihood of side effects. Rather, if the release is slower, the micelles have time to accumulate in the tumor via the EPR effect⁶ before a sizable amount of drug has escaped.

These findings call for replotting the cumulative release data shown in Figure 7 as a function of $t^{1/2}$. A diffusion-controlled release is characteristic of the release proportional to the square root of the time. Therefore, a linear trend is expected, with the diffusivity, or rate of release, approximated by the slope of the line. Indeed, when the paclitaxel release for each polymer is plotted in this manner, as shown in Figure 8, its release trend is approximated for each polymer with lines having two different slopes, strongly suggesting two distinct stages of release. For the diblock, an initially steep slope begins immediately, followed by a leveling off associated with a more gradual release. By the time the release levels off, however, nearly 60% of the drug has been released in just over 4 h; the classic burst release profile typical of most, if not all diblock copolymers. For the PDLLA triblock, the initial slope is also steep, very similar to the initial slope for the diblock, but it does not begin until an hour or so has passed, and ends at a concentration of 50% at around 6–7 h, which means a delayed and hence more reduced burst release profile. For the PLLA triblock, however, following a delay similar to that observed for the PDLLA triblock, only 20% of the drug is released after the initial slope levels off after 6–7 h, which means an ideal, nearly burst-free release profile. However exciting per se, from the drug-delivery standpoint, these factual findings of high drug loading, high drug-encapsulation efficiency, and, above all, the slow, essentially

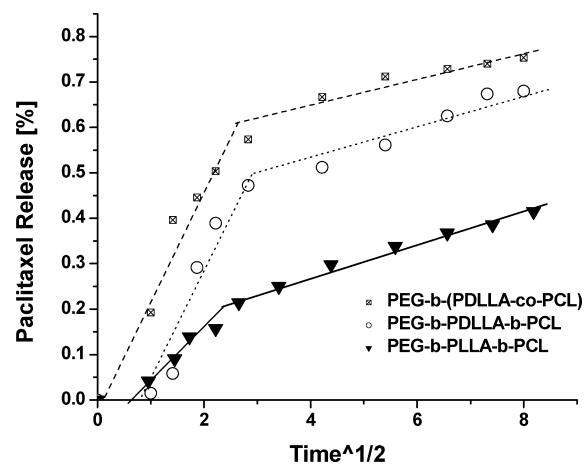


Figure 8. Cumulative paclitaxel release plotted as a function of $t^{1/2}$ for experiments plotted in Figure 7.

burst-free release inspire a few conjectures and provoke even more questions.

For one thing, the data presented in Figures 7 and 8 suggest that the additional block can inhibit paclitaxel diffusion from each triblock relative to the diffusion from the diblock, particularly in the early stages of release. This confirms the hypothesis that a protective layer formed by the middle block around the drug-containing PCL core can indeed inhibit its release, albeit to a different degree. A very interesting question is the release rate difference between the PDLLA and PLLA triblocks. Figure 4 shows that the paclitaxel precipitated after the formation of the PDLLA middle layer. Therefore, this middle layer was not able to act as an additional barrier to inhibit burst drug release. On the other hand, PLLA middle layer formed after paclitaxel precipitated (Figure 5), and thus this layer covered the drug contained core, inhibiting drug burst release (Figure 9).

In order to further explore these concepts, Figure 9 illustrates two block-collapse-induced structure-forming mechanisms along the decompression path for a triblock solution, across four transition lines, from top to bottom—micellization pressure (MP), drug nucleation (around its cloud point), middle layer collapse, and, finally, corona collapse that causes bulk separation from the solvent at the cloud pressure (CP). The path sketched on the right builds on and reflects the common but simplistic belief that 100% of the drug somehow ends up encapsulated in the core immediately upon micellization (as in the liquid titration process). The path sketched on the left reflects a more nuanced and thermodynamically sound conjecture that takes into account two distinct stages of drug interaction with the micelle as it is initiated and transformed in the near-critical solvent. The first stage is in the micellar region between MP and drug CP, when the drug is completely miscible with the solvent, free to interact with the polymer micelles, but still energized with a dense-solvent-induced chemical potential that prevents significant nucleation or aggregation. Even the most rudimentary mean-field thermodynamic analysis, such as that on the basis of approximations derived from statistical associating fluid theory (SAFT),³⁴ suggests that the drug will then partition between the core and solution. By virtue of its high affinity to the core, its mole fraction in the core is likely higher or much higher than that in solution; hence, its affinity-driven “*K*-factor” is high, but the reality of mass balance suggests that much of it must still

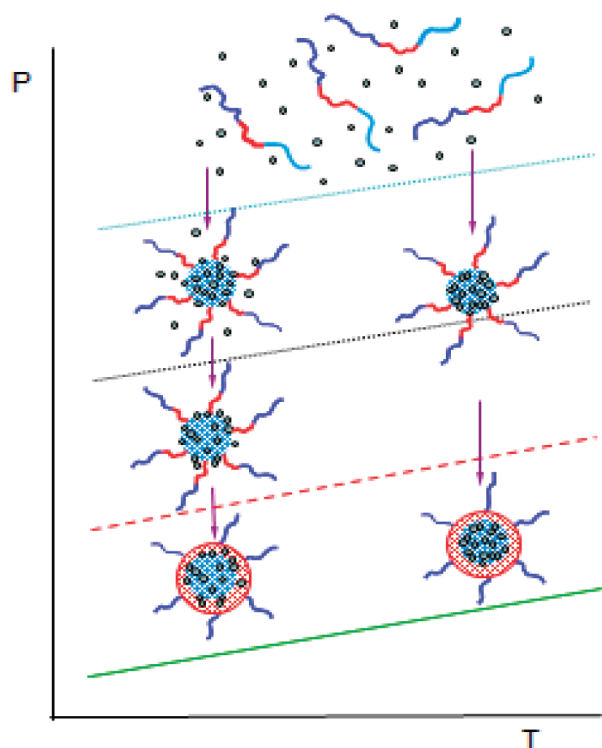


Figure 9. Sequence of block collapse and drug encapsulation upon near-critical micellization.

remain in solution. However, upon further decompression, as such a micellar system approaches and crosses the drug cloud pressure (but before it crosses the PLLA block-collapse pressure), the drug must start nucleating. While normally, in the absence of polymer, the drug will then simply coalesce and precipitate from solution in bulk, now its preferred nucleation and deposition seeds are the micelle cores, to which, we recall, the hydrophobic drug has a much higher affinity than to their coronas. In other words, instead of precipitating from solution in bulk, hence being completely unavailable to micelles, the drug molecules can happily drift to and rest on the micelle core. Upon further decompression, this drug-containing and drug-covered core will now be coated with the middle-block (PLLA) as it reaches its turn to collapse. This sequential-block-collapse and drug-deposition conjecture is consistent with the scattered-light-intensity and drug release data presented in the previous sections.

Regardless of possible explanations, this is a promising lead toward polymeric micellar drug carriers that not only are more drug-efficient, which eliminates the losses of expensive drugs, drug-richer, which reduces the body exposure to the excipient polymer, but also can produce essentially burst-free release, which reduces if not eliminates its toxic side effects. Such a near-critical stepwise-micellization route to reducing burst release can therefore be much more attractive than other approaches, such as cross-linking,¹⁹ which cannot overcome the low drug loading and efficiency challenges. It goes without saying that this preliminary proof of concept inspires plenty of future work, for example, to confirm directly the structural details of the new triblock micelles, say, using transmission electron microscopy (in progress), and to optimize each block size and structure, especially the protective shell-forming block structure, which overflows with biting science questions that

make the near-critical micellization so exciting, especially toward more effective and benign drug formulations.

CONCLUSION

Near-critical micellization (NCM), allowing for precise pressure-tuned control of sequential block collapse and micelle formation, can be synchronized with cancer-drug encapsulation with virtually no drug losses. NCM is demonstrated to produce benign, stable nanoparticles made of PEG-*b*-PLLA-*b*-PCL triblock copolymers that are not only solvent-free and paclitaxel-rich, which reduces the body exposure to the excipients, but also nearly burst-release-free, which reduces if not eliminates its toxic side effects while enhancing its therapeutic efficacy. Ultimately, the ability to control the near-critical fluid phase transitions of the self-organizing block copolymers using pressure opens the door for simple, yet precise, design and preparation of drug and gene delivery and other nanomaterials.

AUTHOR INFORMATION

Corresponding Author

*E-mail: shenyq@zju.edu.cn (Y.S.); radosz@uwyo.edu (M.R.).

Notes

The authors declare no competing financial interest.

ACKNOWLEDGMENTS

The authors give their special thanks to Dr. Erlei Jin for his assistance with the polymer synthesis and characterization.

The authors acknowledge financial support from the U.S. National Science Foundation (CBET-0828472 and CBET-1034530) and National Science Foundation of China Distinguished Young Scholar Award (50888001).

REFERENCES

- (1) Lee, K.; Chung, H.; Im, S.; Park, Y.; Kim, C.; Kim, S. *Breast Cancer Res. Treat.* **2008**, *108*, 241–250.
- (2) Gref, R.; Minamitake, Y.; Peracchia, M.; Trubetskoy, V.; Torchilin, V.; Langer, R. *Science* **1994**, *263*, 1600–1603.
- (3) Kabanov, A.; Alakhov, V. *Micelles of Amphiphilic Block Copolymers as Vehicles for Drug Delivery*; Elsevier: Dordrecht, 1997.
- (4) Kataoka, K.; Harada, A.; Nagasaki, Y. *Adv. Drug Delivery Rev.* **2001**, *47*, 113–131.
- (5) Kwon, G.; Naito, M.; Yokoyama, M.; Okano, T.; Sakurai, Y.; Kataoka, K. *J. Controlled Release* **1997**, *48*, 195–201.
- (6) Maeda, H.; Bharate, G.; Daruwalla, J. *Eur. J. Pharm. Biopharm.* **2009**, *71*, 409–419.
- (7) Farokhzad, O.; Langer, R. *ACS Nano* **2009**, *3*, 16–20.
- (8) Heidel, J.; Davis, M. *Pharm. Res.* **2011**, *28*, 187–199.
- (9) Johnson, B.; Prudhomme, R. *Phys. Rev. Lett.* **2003**, *91* (11), 118302/1–4.
- (10) Heald, C.; Stolnik, S.; De Matteis, C.; Garnett, M.; Illum, L.; Davis, S.; Leermakers, F. *Colloids Surf., A* **2001**, *179*, 79–91.
- (11) Agrawal, S.; Sanabria-DeLong, N.; Coburn, J.; Tew, G.; Bhatia, S. *J. Controlled Release* **2006**, *112*, 64–71.
- (12) Aliabadi, H.; Mahmud, A.; Sharifabadi, A.; Lavasanifar, A. *J. Controlled Release* **2005**, *104* (2), 301–311.
- (13) Zhang, X.; Jackson, J.; Burt, H. *Int. J. Pharm.* **1996**, *132*, 195–206.
- (14) Tyrrell, Z.; Shen, Y.; Radosz, M. *Prog. Polym. Sci.* **2010**, *35*, 1128–1143.
- (15) Huang, X.; Brazel, C. *J. Controlled Release* **2001**, *73*, 121–136.
- (16) Zhang, L.; Hu, Y.; Jiang, X.; Yang, C.; Lu, W.; Yang, Y. *J. Controlled Release* **2004**, *96*, 135–148.
- (17) Shen, Y.; Zhan, Y.; Tang, J.; Xu, P.; Johnson, P.; Radosz, M.; Van Kirk, E.; Murdoch, W. *AIChE J.* **2008**, *54*, 2979–2989.

- (18) Sun, Q.; Radosz, M.; Shen, Y. *J. Controlled Release* **2012**, in press.
- (19) Shuai, X.; Merdan, T.; Schaper, A.; Xi, F.; Kissel, T. *Bioconjugate Chem.* **2004**, *15* (3), 441–448.
- (20) Bae, Y.; Nishiyama, N.; Fukushima, S.; Koyama, H.; Yasuhiro, M.; Kataoka, K. *Bioconjugate Chem.* **2005**, *16*, 122–130.
- (21) Hruby, M.; Konak, C.; Ulbrich, K. *J. Controlled Release* **2005**, *103* (1), 137–148.
- (22) Lee, E.; Na, K.; Bae, Y. *J. Controlled Release* **2003**, *91*, 103–13.
- (23) Choi, C.; Chae, S.; Nah, J. *Polymer* **2006**, *47*, 4571–4580.
- (24) Nakayama, M.; Okano, T.; Miyazaki, T.; Kohori, F.; Sakai, K.; Yokoyama, M. *J. Controlled Release* **2006**, *115*, 46–56.
- (25) Darney, P.; Monroe, S.; Klaisle, C.; Alvarado, A. *Am. J. Obstet. Gynecol.* **1989**, *160*, 1292–1295.
- (26) Tyrrell, Z.; Shen, Y.; Radosz, M. *J. Phys. Chem. C* **2011**, *115*, 11951–11956.
- (27) Middleton, J.; Tipton, A. *Biomaterials* **2000**, *21*, 2335–2346.
- (28) Hu, Y.; Jiang, X.; Ding, Y.; Zhang, L.; Yang, C.; Zhang, J.; Chen, J.; Yang, Y. *Biomaterials* **2003**, *24*, 2395–2404.
- (29) Winoto, W.; Adidharma, H.; Radosz, M. *Macromolecules* **2006**, *39*, 8140–8144.
- (30) Zhao, J.; Allen, C.; Eisenberg, A. *Macromolecules* **1997**, *30*, 7143–7150.
- (31) Tyrrell, Z.; Winoto, W.; Shen, Y.; Radosz, M. *Ind. Eng. Chem. Res.* **2009**, *48*, 1928–1932.
- (32) Edmonds, W.; Hillmyer, M.; Lodge, T. *Macromolecules* **2007**, *40*, 4917–4923.
- (33) Green, J.; Tyrrell, Z.; Radosz, M. *J. Phys. Chem. C* **2010**, *114*, 16082–16086.
- (34) Tan, S.; Winoto, W.; Radosz, M. *J. Phys. Chem. C* **2007**, *111*, 15752–15758.